Kirschner, S., F. Seitz: Recursive adjustment approach for the estimation of physical Earth parameters from polar motion. In: Earth on the Edge: Science for a Sustainable Planet, Rizos, C., P. Willis (Eds.), IAG Symposia, Vol. 139, 453-460, Springer, Berlin, 2014

DOI: 10.1007/978-3-642-37222-3_60

Recursive adjustment approach for the estimation of physical Earth parameters from observations of polar motion

S. Kirschner, F. Seitz
Earth Oriented Space Science and Technology (ESPACE), Technische Universität München, Arcisstr. 21, D-80290 München, Germany

Abstract: The connection between highly precise time series of Earth rotation parameters (ERP) and geophysical processes in the Earth system can be studied on the basis of analytical or numerical forward models. Such models are dependent on a variety of parameters describing geometrical, physical or rheological properties of the Earth. A sensitivity analysis showed that some weakly determined Earth parameters have a large influence on the forward model results. We aim at the improvement of such parameters on the basis of observed ERP. In order to make use of the long ERP time series that cover several decades, a recursive adjustment procedure is being developed. We present the principle of the approach and compare it to a least-squares adjustment in the Gauss-Helmert model. It is shown that both approaches are comparable with respect to the results, but the recursive procedure is superior in terms of computational efficiency. Our study focuses on the pole tide Love number k_2, a specifically critical model parameter that is directly related to period and damping of the modelled Chandler oscillation. In order to simplify the case, the algorithm is developed and tested for a simpler example of a two-dimensional spring mass damper system in which the simulated damped oscillation is equivalent to the Chandler oscillation.

Keywords: Earth rotation, Euler-Liouville equation, pole tide Love number, recursive adjustment, inverse problem

1 Introduction

Variations of Earth rotation with respect to an Earth-fixed reference system are expressed by the Earth rotation parameters (ERP) polar motion and changes of length-of-day. Since many decades space geodesy provides time series of these parameters with increasing accuracy. ERP are influenced by various processes and interactions within and between different subsystems of the Earth. Consequently, dynamic forward modelling of respective effects allows for the investigation of variations of Earth rotation. In forward models time series of ERP or deduced angular momentum functions are balanced with the superposed effects of various driving mechanisms. Among the most important ones are atmospheric and hydrospheric angular momentum variations and solid Earth deformations due to tides, loading and rotational variations.

Previously the Dynamic Model for Earth Rotation and Gravity (DyMEG) (Seitz et al, 2004) has been developed. DyMEG aims at a simulation of ERP on the basis of a consistent balance of external and internal gravitational and geophysical processes. Naturally the quality of the balance also depends on a multitude of physical, rheological and geometrical parameters in DyMEG and underlying models that describe processes in the Earth's subsystems (e.g. atmosphere and ocean models). Many of the model parameters are weakly determined from sparse observations or simplified model assumptions. A sensitivity analysis of DyMEG showed that numerical values of some of these parameters have a significant influence on the model result (Seitz and Kutterer, 2005). Among them, the pole tide Love number k_2 (Section 2) has been identified as the most critical parameter since it directly influences the modelled Chandler oscillation.

Our project aims at the implementation of a reliable adjustment procedure for the estimation and improvement of such parameters. Here we focus on the pole tide Love number k_2. Its numerical value is related to the damping of the Chandler oscillation. Since this damping is very slow (for details see Section 2), observations over a time span of several decades need to be taken into account in order to derive a meaningful value. In order to increase the computational efficiency of the procedure we propose a recursive adjustment procedure. In the following we present the principle of the approach (Section 3) and compare its results to a least-squares adjustment procedure in the Gauss-Helmert model (Section 4). The focus of this paper is on the methodology. Therefore we outline the procedure for the case of a two-dimensional spring mass damper system in order to reduce the complexity of the real situation. The parameters involved (spring constant and damping coefficient) determine period and damping of the simulated oscillation. This way they are comparable to real and imaginary part of pole tide Love number k_2 which makes the simplified example well suited for conclusions with respect to the Chandler oscillation and the estimation of pole tide Love number k_2.

2 Theory of Earth rotation

The physical model of Earth rotation is based on the balance of angular momentum in the Earth system. With respect to an Earth-fixed reference system this balance is described by the well-known Euler-Liouville equation (Lambeck, 1980):

$$\frac{d}{dt}\left(\mathbf{I}\boldsymbol{\omega}+\mathbf{h}\right)+\boldsymbol{\omega}\times\left(\mathbf{I}\boldsymbol{\omega}+\mathbf{h}\right)=\mathbf{L}\ . \qquad (1)$$

The Earth's tensor of inertia $\mathbf{I}$ is influenced by the mass distribution in the Earth system. Vector $\mathbf{h}$ accounts for variations of angular momentum due to the motion of masses with respect to the reference system, and $\mathbf{L}$ stands for external gravitational torques. The Earth rotation vector $\boldsymbol{\omega}$ comprises the small quantities m_1, m_2 and m_2 that are related to polar motion in x- and y-direction and variations of length-of-day respectively:

$$\boldsymbol{\omega}=\Omega\begin{pmatrix} m_1(t)\\ m_2(t)\\ 1+m_3(t)\end{pmatrix}\ . \qquad (2)$$

In this equation $\Omega = 2\pi/86164\ s$ is the angular velocity of the Earth-fixed reference system with respect to which variations of Earth rotation are viewed.

Observed time series of ERP are provided by the International Earth Rotation and Reference Systems Service (IERS) in its C04 series (Dick and Richter, 2009). Variations of length-of-day will not be treated in the following since they are not related to the pole tide Love number k_2 which is our parameter of interest. Observations of polar motion are characterised by a dominant beat between two oscillations, the annual oscillation and the Chandler oscillation. While the annual oscillation is a forced phenomenon that results from the strong annual variability of the mass distribution in the Earth system, the Chandler oscillation is a free rotational mode of the Earth that is caused by the misalignment of the Earth's figure axis and rotation axis. Due to the anelasticity of the Earth's mantle and associated dissipation caused by friction the Chandler oscillation is damped.

Variations of $\mathbf{I}$ and $\mathbf{h}$ are caused by mass redistributions and motions in individual subsystems of the Earth (Fig. 1). Here we focus in particular on the effect of rotational deformations of the solid Earth and the oceans that are caused by time-variable centrifugal forces resulting from polar motion. Physically, the inclusion of rotational deformations means the transition from a rotating rigid to a rotating deformable body. Rotational deformations are responsible for the prolongation of the period of the free oscillation from 304 days (Euler period) to approximately 432 days (Chandler period) and are accompanied by the above-mentioned dissipation (Lambeck, 1980). The deformations give rise to variations of the tensor of inertia and thus yield a back-coupling effect on polar motion.

With respect to principal axis, the tensor of inertia can be formulated explicitly in terms of principal moments of inertia of the Earth (A, B and C) and time-variable surcharges due to mass

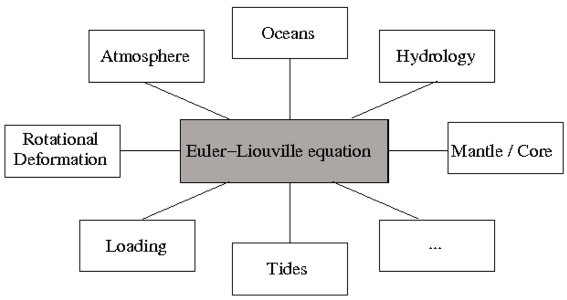

Figure 1: Mass redistributions and motions in the Earth's subsystems influence the balance of angular momentum that is described by the Euler-Liouville equation.

variations in the different subsystems ($c_{ij};\ i,j = 1,2,3$):

$$I = \begin{bmatrix} A + c_{11} & c_{12} & c_{13} \\ c_{12} & B + c_{22} & c_{23} \\ c_{13} & c_{23} & C + c_{33} \end{bmatrix} \tag{3}$$

$$c_{ij} = c_{ij}^{atmosphere} + c_{ij}^{ocean} + c_{ij}^{rotdef} + \dots \ .$$

Here c_{ij}^{rotdef} describes the effect of rotational deformations. In particular, the two tensor elements c_{13} and c_{23} are related to the corresponding mass redistributions (Lambeck, 1980):

$$\begin{aligned} c_{13}^{rotdef} &= \frac{\Omega^2 \cdot a^5}{3 \cdot G} \left(\Re\left(k_2\right) \cdot m_1 + \Im\left(k_2\right) \cdot m_2 \right) \\ c_{23}^{rotdef} &= \frac{\Omega^2 \cdot a^5}{3 \cdot G} \left(\Re\left(k_2\right) \cdot m_1 - \Im\left(k_2\right) \cdot m_2 \right) \ . \end{aligned} \tag{4}$$

In these equations the dimensionless pole tide Love number $k_2 = \Re\left(k_2\right) + \Im\left(k_2\right) i$ ($i = \sqrt{-1}$) describes the anelasic response of the Earth's body and the ocean to polar motion, a is the Earth's semi major axis and G means the gravitational constant. The real part of k_2 is connected with the period of the Chandler oscillation, and the imaginary part with its damping (cf. Seitz and Kutterer (2005) for details). Since k_2 is characterised by a high level of uncertainty (see Tab. 6.1 in Seitz and Schuh (2010) for a review of different values that can be found in the literature) and at the same time one of the central parameters for modelling the Chandler oscillation, we aim at an improvement of this parameter within our adjustment approach. It shall be assumed in this study that all other sources of mass redistributions and motions in the Earth system are known and perfectly described by the model. This simplification has of course to be kept in mind, and further studies will have to address the validity of the results of the estimation procedure in the light of the accuracy of model components and other parameters. This is, however, beyond the scope of the present paper.

The result of a simulation with DyMEG over 100 years in which solely the effects of rotational deformations were considered is shown in Figure 5 of Seitz and Schuh (2010). All other mass redistributions and motions in the Earth system as well as external torques were neglected. The resulting oscillation (Chandler oscillation) with a period of 431.9 is clearly damped, and after 22 years its amplitude is reduced by half. The value of $k_2 = 0.35 + 0.0036i$ used in this experiment was taken from the Conventions of the IERS 2003 (McCarthy and Petit, 2004). It corresponds to a damping coefficient of $Q = 82$ and is representative for a deformable Earth with a spherical liquid core including the effects of ocean pole tides and mantle anelasticity.

In order to develop our adjustment approach we simplify the problem at hand by replacing the Chandler oscillation modelled via DyMEG by a simple damped oscillation from a two-dimensional spring mass damper system. Such a system creates a damped two dimensional circular motion that is fully equivalent to the damped Chandler oscillation of the Earth. Parameters that need to be defined in this system are the spring constant and the damping coefficient that determine period and damping of the simulated oscillation in analogy to real and imaginary part of k_2. Therefore the results from this study are later on directly applicable for the inversion of DyMEG.

3 Adjustment approach

Figure 2 displays the set-up of our spring mass damper system in a principle sketch. It is assumed that the damped motion is circular which holds also for the modelled Chandler oscillation. The displacement **z** of the two-dimensional system is a vector containing the respective displacements in x- and y-direction. The damping coefficient is denoted by b. It corresponds to $\Im\left(k_2\right)$ in the case of the Chandler oscillation. The spring constant, that corresponds to $\Re\left(k_2\right)$ is denoted by k. The mass m is set to 1 kg.

The resulting damped oscillation is described

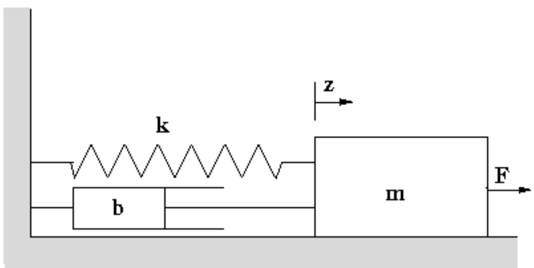

Figure 2: Sketch of the Spring mass damper system.

by following differential equation:

$$\ddot{\mathbf{z}} = \frac{k}{m}\mathbf{z} - \frac{b}{m}\dot{\mathbf{z}} \ . \tag{5}$$

We simulate the time-dependent displacement with

$$\mathbf{z} = \begin{bmatrix} x \\ y \end{bmatrix} = \begin{bmatrix} x_0 \cdot e^{-\frac{b}{2}t} \ sin(\omega \cdot t) \\ y_0 \cdot e^{-\frac{b}{2}t} \ cos(\omega \cdot t) \end{bmatrix} \ , \tag{6}$$

where x_0 and y_0 are the initial values of the oscillation and the angular frequency is $\omega = \sqrt{\frac{k}{m} - \frac{b^2}{4m^2}}$. Figure 3 shows the simulated damped two-dimensional oscillation (period: 10.62 s). This simulation represents the observations in the adjustment approach.

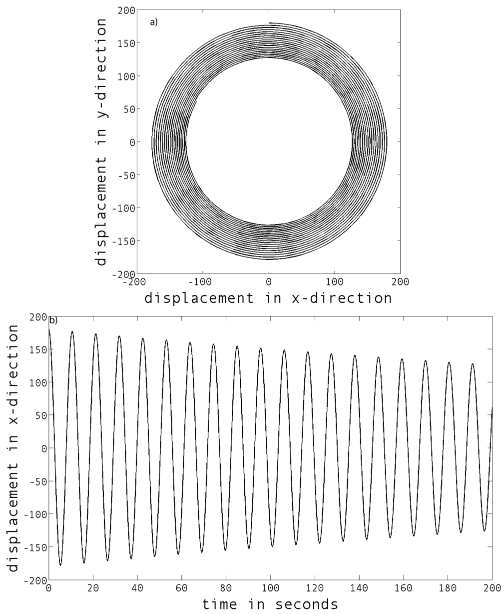

Figure 3: Simulated oscillation of the spring mass damper system. Parameters: $x_0 = 180$, $y_0 = 180$, $k = 0.35$, $b = 0.0036$, $m = 1$ kg; a) displacement in x- and y-direction; b) oscillation in x-direction; the oscillation in y-direction is similar with a phase-shift of $\frac{\pi}{2}$.

3.1 Parameter estimation in the Gauss-Helmert Model

An appropriate approach for estimating the spring parameters (and in analogy for the pole tide Love number k_2) from the observations is the least-squares adjustment in the Gauss-Helmert Model. This approach matches the problem at hand in which unknowns ($\mathbf{x} = \begin{bmatrix} k & b \end{bmatrix}$) and observations $\mathbf{z}$ cannot be separated. The functional model $\mathbf{F}(\mathbf{z}, \mathbf{x})$ of the approach has the form (Niemeier, 2008):

$$\mathbf{F}(\mathbf{z}, \mathbf{x}) = \mathbf{A} \cdot \Delta\mathbf{x} + \mathbf{B} \cdot \mathbf{v} + \mathbf{w} = 0 \ . \tag{7}$$

Here $\mathbf{A}$ and $\mathbf{B}$ are design matrices (Eqs. 9 and 10), $\Delta\mathbf{x}$ is the improvement of the unknowns relative to initial values and $\mathbf{v}$ is the vector of the residuals. The discrepancy vector $\mathbf{w}$ is calucu-lated via the functional model by inserting initial values for the unknowns and the observations.

For the linearisation of the differential equation that describes the motion of the spring mass (Eq. 5) first and second derivative of the displacement $\mathbf{z}$ are approximated by central difference quotients (the central difference quotient is known to be more stable and accurate than the forward or backward difference quotient). Consequently the functional model is represented by the linearised equations

$$\begin{aligned} x_{k-2} - \frac{2tb}{m}x_{k-1} + \left(\frac{4t^2k}{m} - 2\right)x_k + \frac{2tb}{m}x_{k+1} + x_{k+2} = 0 \\ y_{k-2} - \frac{2tb}{m}y_{k-1} + \left(\frac{4t^2k}{m} - 2\right)y_k + \frac{2tb}{m}y_{k+1} + y_{k+2} = 0 \ . \end{aligned} \tag{8}$$

The design matrices $\mathbf{A}$ and $\mathbf{B}$ mean the partial derivatives of the functional model with respect to unknowns and observations:

$$\mathbf{A} = \left[\frac{\partial \mathbf{F}(\mathbf{z}, \mathbf{x})}{\partial \mathbf{x}}\right] = \left[\frac{\partial \mathbf{F}(\mathbf{z}, \mathbf{k})}{\partial \mathbf{k}} \quad \frac{\partial \mathbf{F}(\mathbf{z}, \mathbf{b})}{\partial \mathbf{b}}\right] \tag{9}$$

$$\begin{aligned} \mathbf{B} &= \left[\frac{\partial \mathbf{F}(\mathbf{z}, \mathbf{x})}{\partial \mathbf{z}}\right] = \begin{bmatrix} \mathbf{B1} & \mathbf{0} \\ \mathbf{0} & \mathbf{B2} \end{bmatrix} \ , \ \text{with} \\ \mathbf{B1} &= \left[\frac{\partial \mathbf{F}}{\partial x_{k-2}} \quad \frac{\partial \mathbf{F}}{\partial x_{k-1}} \quad \frac{\partial \mathbf{F}}{\partial x_k} \quad \frac{\partial \mathbf{F}}{\partial x_{k+1}} \quad \frac{\partial \mathbf{F}}{\partial x_{k+2}}\right] \\ \mathbf{B2} &= \left[\frac{\partial \mathbf{F}}{\partial y_{k-2}} \quad \frac{\partial \mathbf{F}}{\partial y_{k-1}} \quad \frac{\partial \mathbf{F}}{\partial y_k} \quad \frac{\partial \mathbf{F}}{\partial y_{k+1}} \quad \frac{\partial \mathbf{F}}{\partial y_{k+2}}\right] \ . \end{aligned} \tag{10}$$

For the spring mass damper system we obtain:

$$\mathbf{A} = \begin{bmatrix} \frac{4t^2}{m}x_k & -\frac{2t}{m}x_{k-1} + \frac{2t}{m}x_{k+1} \\ \frac{4t^2}{m}y_k & -\frac{2t}{m}y_{k-1} + \frac{2t}{m}y_{k+1} \end{bmatrix} \tag{11}$$

$$\mathbf{B1} = \mathbf{B2} = \begin{bmatrix} 1 & -\frac{2tb}{m} & \frac{4t^2k}{m} & \frac{2tb}{m} & 1 \end{bmatrix} \ . \tag{12}$$

The structure of the $\mathbf{B}$-matrix is displayed in Figure 4. According to Niemeier (2008) $\Delta\mathbf{x}$ is estimated by

$$\Delta\mathbf{x} = -\left(\mathbf{A}^T\left(\mathbf{B}\mathbf{Q}_{ll}\mathbf{B}^T\right)^{-1}\mathbf{A}\right)^{-1}\mathbf{A}^T\left(\mathbf{B}\mathbf{Q}_{ll}\mathbf{B}^T\right)\mathbf{w} \tag{13}$$

where $\mathbf{Q}_{ll}$ is a weighting matrix. In our simulation we apply an identity matrix assuming laboratory conditions without measurement errors. For the case of Earth rotation the (time-variable) accuracy of geodetic observations would have to be taken into account. The cofactor matrix of the unknowns is given by

$$\mathbf{Q}_{xx} = \left(\mathbf{A}^T \left(\mathbf{B}\mathbf{Q}_{ll}\mathbf{B}^T\right)^{-1} \mathbf{A}\right)^{-1} . \quad (14)$$

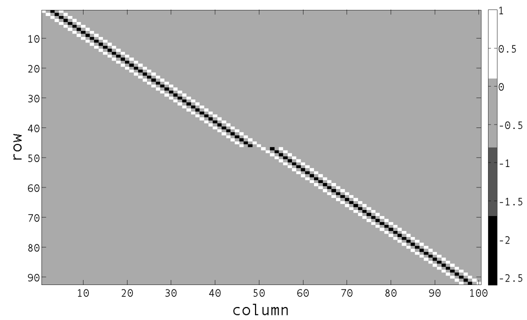

Figure 4: **B**-matrix for 50 observations.

3.2 Recursive adjustment

More efficiently the parameter estimation can be performed in a recursive procedure (Kutterer and Neumann, 2010). It allows a fast calculation and requires less segmentation capacity than the standard adjustment approach in the Gauss-Helmert Model. The difference with respect to the latter is, that after an initial estimate using a certain number of observations stepwise only one new observation i $(i = 1, 2, 3, ...)$ is considered:

$$\mathbf{w}^i + \mathbf{B}^i \cdot \mathbf{v}^i + \mathbf{A}^i \cdot \Delta\mathbf{x}^i = 0 . \quad (15)$$

The estimated unknowns from the previous step are considered as additional observations. Therefore the functional model is extended into

$$\begin{bmatrix}\mathbf{w}^i \\ 0\end{bmatrix} \begin{bmatrix}\mathbf{B}^i & 0 \\ 0 & I\end{bmatrix} \cdot \begin{bmatrix}\mathbf{v}^i \\ v^{i-1}\end{bmatrix} + \begin{bmatrix}\mathbf{A}^i \\ I\end{bmatrix} \cdot \Delta\mathbf{x}^i = 0 . \quad (16)$$

This way the inversion has to be performed only for the new observation in each step:

$$\Delta\mathbf{x}^i = \mathbf{A}^{i^T} \left(\mathbf{B}^i\mathbf{Q}^i_{ll}\mathbf{B}^{i^T}\right)^{-1} \mathbf{Q}^i_{xx}\ \mathbf{w}^i \quad (17)$$

$$\mathbf{Q}^i_{xx} = \left(\mathbf{A}^{i^T} \left(\mathbf{B}^i\mathbf{Q}^i_{ll}\mathbf{B}^{i^T}\right)^{-1} \mathbf{A}^i + \left(\mathbf{Q}^{i-1}_{xx}\right)^{-1}\right)^{-1} . \quad (18)$$

This procedure allows a fast computation and, consequently, longer observation series may be used for the estimation of the parameters. This is especially useful for the computation of the damping coefficient. Since the damping is comparable slow a longer time-series can significantly improve the accuracy of the estimate.

4 Results

4.1 Adjustment in the Gauss-Helmert Model

The estimation is performed for a time-span of 200 s (cf. Fig. 3). The results turn out to be very sensitive to the sampling rate of the data as a consequence of the applied central difference quotient (Tab. 1). For small sampling rates the approximation of the first and second derivative of the displacement is more accurate. The result is especially influenced by the approximation of the first derivative that is calculated on the basis of three observations. The second derivative is more accurate since it is based on five observations.

Since we assumed error-free conditions so far, the estimates of both unknown parameters are highly precise. Standard deviations are in the order of 10^{-14}. The comparison of the results with the values that have been applied in the simulation ($k = 0.35$, $b = 0.0036$) shows a very good agreement for sampling rates of about 0.1 s and smaller. For this value the differences between original value and estimate are $4.1 \cdot 10^{-4}$ for the spring constant k and $1.6 \cdot 10^{-5}$ for the damping coefficient b. The limit of the segmentation capacity of a standard PC is exceeded if a sampling rate of 0.01 s is applied for a 200 s time-span. Under error-free conditions of course a shortening of the time-span is possible and does not change the results much. However (as will be shown below) the length of the simulation becomes very important as soon as noise is added to the observations.

sampling rate in seconds	k	b
0.05	0.3498979	0.0035984
0.10	0.3495919	0.0035937
0.50	0.3399102	0.0034436
1.00	0.3110260	0.0029882

Table 1: Estimates of the unknown parameters for different sampling rates.

4.2 Recursive approach

The estimates from the recursive approach are identical to those of the adjustment in the standard Gauss-Helmert Model. Differences are only visible in the fourteenth or fifteenth decimal place due to rounding errors. However the processing times are very different (Tab. 2). Here we used 50 observations in the initial step of the recursive procedure. As outlined above, one additional observation is added in each subsequent step. The comparison of the computation times reveals that the recursive adjustment method is much more efficient which holds especially for longer observation series. In contrast to the standard approach the recursive adjustment allows for the application of very high sampling rates. For a sampling of 0.01 s of our 200 s time-span we obtain the values $k = 0.3499959$ and $b = 0.0035999$; the computation requires only 1.77 s.

sampling rate in seconds	t_{proc} in seconds	t_{proc}^{rec} in seconds	number of observations
0.05	854.02	0.51	4001
0.10	100.56	0.40	2001
0.50	2.28	0.15	401
1.00	0.23	0.15	201

Table 2: Comparison of the processing times on a 32 bit processor for the standard Gauss-Helmert Model (t_{proc}) and for the recursive approach (t_{proc}^{rec}).

4.3 Considering observation errors

Now we perform an experiment with normal distributed random noise added to the observations. The noise level is chosen to be 10^{-4} of the (mean) amplitude of the damped oscillation which corresponds to the accuracy of the ERP (mean Chandler amplitude: 170 mas; observation accuracy: 0.1 mas). The recursive approach is applied to two simulated oscillations of 20 s and 2000 s length (sampling rate: 0.1 s). For the longer time series the standard deviation σ of both estimated parameters is clearly smaller, and in particular the result for the damping coefficient is closer to the original value (Tab. 3). From this experiment we conclude that the application of the procedure to a long ERP time series will be beneficial.

length of time series in seconds	20	2000
k	0.3495921	0.3495466
σ_k	0.0000319	0.0000136
b	0.0035937	0.0035993
σ_b	0.0000539	0.0000217

Table 3: Estimates of the unknown parameters for oscillations over different time-spans with corresponding standard deviations σ.

5 Conclusion & Discussion

The results from the previous section show that the recursive procedure is an efficient and reliable method for the estimation of parameters from long time series. Furthermore it has been demonstrated that the estimates of the spring parameters from noisy observations improve with the length of the time series.

For our problem at hand we found out that a sampling rate of at least 0.1 s is necessary in order to obtain satisfying results. The period of the simulated oscillation was 10.62 s, which means that we require more than 100 samples per period. For the Chandler oscillation with a period of 432 days this would mean in analogy that we require a temporal resolution of a few days (which is unproblematic since daily values of ERP are provided). Meanwhile highly accurate observations of polar motion are available for five decades. In conclusion we expect a stable estimate of the pole tide Love number k_2 when the recursive procedure is applied to ERP. The results will be discussed in a follow-up paper to this study.

Acknowledgements: This study is part of project P9 supported by the German Research Foundation (DFG) within Research Unit FOR 584 *Earth Rotation and Global Dynamic Processes.*

References

Dick W, Richter B (eds) (2009) IERS Annual Report 2007, BKG, Fankfurt

Kutterer H, Neumann I (2010) Recursive least-squares estimation in case of interval observation data. In: Beer M, Muhanna RL, Mullen RL (eds) Observing our Changing Earth, Proc. 4th International Workshop REC 2010, Research Publishing, Singapore, pp 101–116

Lambeck K (1980) The Earth's Vaiable Rotation: Geophysical Causes and Consequences, Cambridge University Press

McCarthy D, Petit G (eds) (2004) IERS Conventions 2003, IERS TN 32, BKG, Fankfurt

Niemeier W (2008) Ausgleichungsrechnung, de Gruyter

Seitz F, Kutterer H (2005) Sensitivity analysis of the non-linear liouville equation. In: Sansò F (ed) A Window on the Future of Geodesy, IAG Symposia, Springer, vol 128, pp 601–606, DOI 10.1007/3-540-27432-4_102

Seitz F, Schuh H (2010) Earth rotation. In: Xu G (ed) Sciences of Geodesy I, Springer, pp 185–227, DOI 10.1007/978-3-642-11741-1_6

Seitz F, Stuck J, Thomas M (2004) Consistent atmospheric and oceanic excitation of the Earth's free polar motion. Geophys J Int 157(1):25–35, DOI 10.1111/j.1365-246X.2004.02208.x